Journal of Quality Measurement and Analysis *JQMA* 21(2) 2025, 163-174
e-ISSN: 2600-8602 *http://www.ukm.my/jqma*
https://doi.org/10.17576/jqma.2102.2025.12

ENHANCED HEAT TRANSFER IN HYBRID NANOFLUID: ROLE OF SUCTION AND WEDGE ANGLE ON BOUNDARY LAYER DYNAMICS

(Peningkatan Pemindahan Haba dalam Nanobendalir Hibrid: Peranan Sedutan dan Sudut Baji Terhadap Dinamik Lapisan Sempadan)

NURUL AMIRA ZAINAL*, ROSLINDA NAZAR, HARIS ALAM ZUBERI & IOAN POP

ABSTRACT

This study offers a numerical investigation of steady MHD flow and heat transfer characteristics of hybrid nanofluids past a permeable stretching/shrinking wedge. The study considers the effect of suction as well as an internal heat source. Similarity transformations are applied to convert the governing partial differential equations into a system of ordinary differential equations and solved numerically using MATLAB's bvp4c function. The results reveal the existence of dual solutions for suction and shrinking parameters over certain ranges. Besides, the study also illustrates that increasing both the suction parameter and the wedge angle resulted in a higher Nusselt number which implies an enhancement in the heat transfer rate.

Keywords: suction; wedge angle; shrinking sheet; hybrid nanofluids; MHD

ABSTRAK

Kajian ini menawarkan penyelidikan berangka mengenai aliran malar MHD dan ciri pemindahan haba nanobendalir hibrid pada permukaan baji meregang/mengecut. Kajian ini mempertimbangkan kesan sedutan serta sumber haba dalaman. Penjelmaan keserupaan digunakan untuk menukarkan persamaan pembezaan separa yang kemudian dijelmakan kepada sistem persamaan pembezaan biasa dan diselesaikan secara kaedah berangka melalui aplikasi fungsi bvp4c dalam MATLAB. Hasil kajian menunjukkan wujud penyelesaian dual bagi parameter sedutan dan pengecutan dalam julat tertentu. Selain itu, kajian ini juga menggambarkan bahawa dengan meningkatkan kedua-dua parameter sedutan dan sudut baji, nombor Nusselt akan menjadi lebih tinggi, seterusnya menunjukkan peningkatan dalam kadar pemindahan haba.

Kata kunci: sedutan; sudut baji; permukaan mengecut; nanobendalir hibrid; MHD

1. Introduction

The pursuit of enhanced heat transfer efficiency has led to the study and development of significant hybrid nanofluids. A nanofluid generally comprises of a base fluid containing suspended nanoparticles. These fluids are expected to offer greater heat transfer rate than the conventional fluids. The early efforts were focused on more single component-based nanofluids which basically improved the heat transfer (Yu *et al.* (2008); Kakaç & Pramuanjaroenkij (2009); Nazari *et al.* (2018)). However, the advancements were rather modest, and subsequently attention was directed to hybrid nanofluids, composed of two or more distinct nanoparticles to achieve the highly desired dual effect of improved thermal conductivity and heat transfer. The range of possible nanoparticles i.e. metallic –copper (Cu), aluminium (Al) (Smrity & Yin (2024)), metal oxides -alumina (Al_2O_3), titanium oxide (TiO_2) (Zainal *et al.* (2024)), or carbon-based – carbon nanotubes (CNTs), graphene (Jin *et al.* (2021)) is very important because they possess the characteristics that are necessary for such applications. The used of hybrid nanofluid in real-application has been recognised in thermal management. Potential applications, such as cooling technologies for electronic devices,

enhancement of energy efficiency in heat exchangers, and biomedical applications like targeted drug delivery and hyperthermia treatment has been studied by Tanveer *et al.* (2025).

In addition, whether a two-step or one-step approach is employed to synthesize the nanoparticles is very important in deciding the stability and effectiveness of the nanofluid. According to Sidik *et al.* (2017), for optimum effectiveness, the homogeneity of the nanofluid, and stability over time should be ensured as agglomeration reduces efficacy. Diverse techniques have been employed to improve stability, such as using surfactants or functionalizing nanoparticles (Guerrini *et al.* (2018)). Moreover, the transfer of heat through hybrid nanofluids has been well documented within several different shapes and flow configurations, as well as combinations of various nanoparticles regarding their thermal performance in stretching/shrinking surfaces. Researchers often use numerical techniques to solve the governing equations that make up the momentum and energy equations with appropriate boundary conditions. Such studies can be found in Abbasi and Farooq (2020), Khan *et al.* (2022), and Kolsi *et al.* (2024).

The inclusion of a magnetic field or magnetohydrodynamic (MHD) further adds to the richness of the flow dynamic and heat transfer. A magnetic field adds Lorentz forces which modifies the velocity and temperature distribution of the fluid. MHD can be simplified as the study of movement of fluids that can conduct electricity inside a magnetic field. The interaction between the motion of fluid and the electromagnetic fields can influence heat and mass transfer mechanisms. Works such as Hartmann and Lazarus (1937) illustrated how a magnetic field could alter the flow of fluids. Later Heiser and Shercliff (1965); Moreau (1990) advanced the understanding of the governing equations of MHD flow and boundary conditions to analyze the possibilities of using magnetic fields to control and improve the heat exchanges in the systems with fluids. Many researchers have concentrated on the effect of MHD on heat transfer processes using hybrid nanofluids over stretching/shrinking surfaces (Mahariq *et al.* (2024); Qureshi *et al.* (2021)). These researches emphasize the combined effect of nanoparticle concentration and stretching/shrinking rate on the enhancement of heat transfer with the existence of MHD. The findings often show that a properly applied magnetic field can increase heat transfer from hybrid nanofluids even more.

The role of suction effects in hybrid nanofluids boundary layer flow is noted as a novel phenomenon in heat transfer. It is observed that an extensive literature exists on the boundary layer flow of nanofluids with suction but a thorough study is needed on the region including hybrid nanofluids. A suction/injection effect had previously been investigated in studies that were mainly concerned with the boundary layer flows of single-phase fluids (Rohni *et al.* (2012); Pandey & Kumar (2016)). These studies establish the basic principles of suction's role in controlling boundary layer thickness, drag forces, and heat transfer rates. Suction enhances the heat transfer by removing the fluid that is close to the surface resulting into thinner boundary layers; which helps in attaining better heat transfer by preventing bulge in the boundary layer. The significance of this effect becomes even more pronounced in the case of unfavorable pressure gradients or high heat transfer coefficients at the surface.

The suite of wedge-shaped surfaces also adds a degree of geometric complexity to the flow dynamics and thermal characteristics. Sakiadis (1961) and Crane (1970) were the pioneer scholars who laid the groundwork for understanding the development of a boundary layer in stretching surfaces. More recent works have begun to expand on such studies to include the problems that wedge geometries present. MHD effects and hybrid nanofluids over stretching or shrinking wedges interact under the influence of surface geometry, distribution of nanoparticles, thermal radiation and external forces. For example, the suction or injection at the wedge surface influences the boundary layer's structure, affecting the heat transfer rate. Such systems have been investigated by Ishak *et al.* (2007), Atalik and Sönmezler (2011) and

Ghosh and Mukhopadhyay (2022) numerically, who observed that under different boundary conditions, the use of nanofluids and magnetic fields improves heat transfer in the systems.

According to the previously stated literature, a gap of study exists in the comprehensive understanding of the optimal combination of nanoparticle types, wedge angle parameters and suction strengths for maximizing heat transfer in hybrid nanofluids. Further research is needed to explore the effects of the parameters as mentioned above, including the concentration of nanoparticles, the suction impact, and the surface geometry, on the boundary layer behaviour and heat transfer performance. This important discovery could further our understanding of this field of study because of the high practical interest in the flow behaviour of the wedge-shaped boundary layer. Moreover, a deeper understanding of these complex interactions is vital for the successful implementation of hybrid nanofluids in advanced heat transfer applications.

2. Mathematical Model

Figure 1 illustrates a steady hybrid alumina-copper nanofluids (Al_2O_3-Cu/H_2O) with suction and magnetic impact past a stretching/ shrinking wedge. The free-stream velocity is assumed to be $u_\infty = U_\infty x^{\vartheta}$ and the velocity as the wedge surface is stretched or shrunk is referred to as $u_w(x) = U_w x^{\vartheta}$, where $U_w < 0$ and $U_w > 0$ denote as shrinking wedge and the stretching wedge, respectively and U_∞ is a positive constant. $B(x)$ is introduced as a magnetic field towards $y-$ axis where $B(x) = B^* x^{(\vartheta-1)/2}$ (B^* is the applied magnetics field strength). The wedge angle is represented by $\vartheta = \beta/(2-\beta)$ where β is Hartree pressure gradient. The value of ϑ is established within $0 < \vartheta < 1$ representing wedge problem. The fluid's ambient temperature can be represented as T_∞ and the temperature of the stretching/shrinking wedge is T_w. Each of the temperatures is assumed to remain constant. This study assumes that the size of the nanoparticles is uniform.

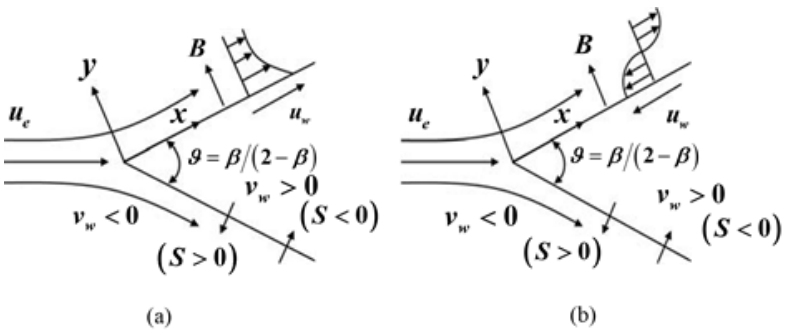

Figure 1: (a) Shrinking wedge and (b) stretching wedge coordinate system

Based on the assumptions made earlier, we can express the mathematical representation as (Tiwari & Das (2007); Awaludin *et al.* (2018)):

$$\frac{\partial u}{\partial x} + \frac{\partial v}{\partial y} = 0, \tag{1}$$

$$u\frac{\partial u}{\partial x} + v\frac{\partial u}{\partial y} = u_\infty \frac{du_\infty}{dx} + \frac{\mu_{hnf}}{\rho_{hnf}}\frac{\partial^2 u}{\partial y^2} + B^2\frac{\sigma_{hnf}}{\rho_{hnf}}(u_\infty - u), \tag{2}$$

$$u\frac{\partial T}{\partial x}+v\frac{\partial T}{\partial y}=\frac{k_{hnf}}{\left(\rho C_p\right)_{hnf}}\frac{\partial^2 T}{\partial y^2}+\frac{Q_0}{\left(\rho C_p\right)_{hnf}}\left(T_\infty - T\right). \tag{3}$$

where

$$\begin{aligned} &u=u_w\left(x\right), v=v_w\left(x\right), T=T_w, \quad \text{at} \quad y=0,\\ &u\to u_\infty\left(x\right),\ T\to T_\infty\left(x\right), \qquad \text{as} \quad y\to\infty. \end{aligned} \tag{4}$$

u and v is a component of the velocity along $x-$ and $y-$ directions, respectively, the velocity of the wall mass transfer is presented as $v_w\left(x\right)$, and the heat absorption/generation variable is $Q_0=Q^* u_\infty x^{(\vartheta-1)}$ with constant Q^*. Table 1 illustrates the thermophysical characteristics of fluid systems, as detailed by Oztop and Abu-Nada (2008), whereas the hybrid nanofluids correlation coefficient is shown in Table 2, according to Raza *et al.* (2016).

Next, the following variables of similarity were adopted (Sparrow *et al.* (1963));

$$\psi=\left(U_\infty \nu_f\right)^{\frac{1}{2}} x^{\frac{(\vartheta+1)}{2}} f\left(\eta\right),\ \eta=\left(U_\infty/\nu_f\right)^{\frac{1}{2}} x^{\frac{(\vartheta-1)}{2}} y,\ \theta\left(\eta\right)=\frac{T-T_\infty}{T_w-T_\infty}, \tag{5}$$

thus,

$$v_w=-\frac{\vartheta+1}{2}\left(U_\infty \nu_f\right)^{\frac{1}{2}} x^{\frac{(\vartheta-1)}{2}} S, \tag{6}$$

where S is the mass flux parameter with $S>0$ for suction and $S<0$ for injection, meanwhile ν_f is the kinematic viscosity of fluid. Next, with the help of similarity transformations presented in the relations (5) and (6), the boundary value problem defined by Eqs. (2), (3), and (4) is systematically transformed into the following ordinary differential equations as follows

$$\frac{\mu_{hnf}/\mu_f}{\rho_{hnf}/\rho_f} f'''+\frac{1+\vartheta}{2} ff''+\vartheta\left(1-f'^2\right)+\frac{\sigma_{hnf}/\sigma_f}{\rho_{hnf}/\rho_f} M\left(1-f'\right)=0, \tag{7}$$

$$\frac{1}{\mathrm{Pr}}\left(\frac{k_{hnf}/k_f}{\left(\rho C_p\right)_{hnf}/\left(\rho C_p\right)_f}\right)\theta''+\frac{1+\vartheta}{2} f\theta'+\frac{1}{\left(\rho C_p\right)_{hnf}/\left(\rho C_p\right)_f} H\theta=0, \tag{8}$$

$$\begin{aligned} &f\left(0\right)=S, f'\left(0\right)=\lambda,\ \theta\left(0\right)=1,\\ &f'\left(\eta\right)\to 1,\ \theta\left(\eta\right)\to 0, \end{aligned} \tag{9}$$

where the magnetic coefficient is presented by $M=\sigma_f B^{*2}/\rho_f U_\infty$, the Prandtl number is $\mathrm{Pr}=\nu_f/\alpha_f$ and the parameter which describes stretching or shrinking in the wedge is

described as $\lambda = U_w / U_\infty$. The parameter of absorption or generation of heat is denoted by $H = Q^* / \left(\rho C_p\right)_f$.

Table 1: The fluid thermophysical properties (Oztop & Abu-Nada 2008)

Characteristic	$\rho\left(\text{kg/m}^3\right)$	$k\left(\text{W/mK}\right)$	$C_p\left(\text{J/kgK}\right)$
H_2O	997.1	0.613	4179
Al_2O_3	3970	40	765
Cu	8933	400	385

Table 2: The correlation coefficient (Raza *et al*. 2016)

Properties	Alumina-Copper/Water
Thermal capacity	$\left(\rho C_p\right)_{hnf} = \phi_1\left(\rho C_p\right)_{s1} + \phi_2\left(\rho C_p\right)_{s2} + \left(1-\phi_{hnf}\right)\left(\rho C_p\right)_f$
Thermal expansion	$\beta_{hnf} - \left(1-\phi_{hnf}\right)\beta_f = \phi_1\beta_{s1} + \phi_2\beta_{s2}$
Thermal conductivity	$\dfrac{k_{hnf}}{k_f} = \left[\dfrac{\left(\dfrac{\phi_1 k_{s1} + \phi_2 k_{s2}}{\phi_{hnf}}\right) + 2k_f + 2\left(\phi_1 k_{s1} + \phi_2 k_{s2}\right) - 2\phi_{hnf} k_f}{\left(\dfrac{\phi_1 k_{s1} + \phi_2 k_{s2}}{\phi_{hnf}}\right) + 2k_f - \left(\phi_1 k_{s1} + \phi_2 k_{s2}\right) + \phi_{hnf} k_f}\right]$ where $\phi_{hnf} = \phi_1 + \phi_2$
Dynamic viscosity	$\mu_{hnf} = \mu_f / \left(1-\phi_{hnf}\right)^{2.5}$
Density	$\rho_{hnf} = \phi_1\rho_{s1} + \phi_2\rho_{s2} + \left(1-\phi_{hnf}\right)\rho_f$

The quantities of interest in this case are the local Nusselt number $Nu_x = \dfrac{x k_{hnf}}{k_f\left(T_w - T_\infty\right)}\left(-\dfrac{\partial T}{\partial y}\right)_{y=0}$, and the skin friction coefficient $C_f = \dfrac{\mu_{hnf}}{\rho_f u_\infty{}^2}\left(\dfrac{\partial u}{\partial y}\right)_{y=0}$. Employing the above-mentioned information we finally derive

$$\text{Re}_x^{1/2} C_f = \frac{\mu_{hnf}}{\mu_f} f''(0), \quad \text{Re}_x^{-1/2} Nu_x = -\frac{k_{hnf}}{k_f}\theta'(0), \tag{10}$$

where $\text{Re}_x = u_\infty(x)x/\nu_f$.

3. Results and Discussion

This section thoroughly discussed the findings obtained from the numerical approach. The computational efficiency of the numerical solution is assessed by evaluating the solver performance and computational cost. The bvp4c solver in MATLAB is used to solve the

transformed boundary layer equations, efficiently. The average computational time varied between 0.5 and 1.2 seconds per iteration, depending on parameter values such as the suction, S and wedge angle, ϑ parameter. Higher values of S generally required more computational resources due to stronger boundary layer effects. The numerical results obtained are consistent with previous studies, confirming the reliability of the solver. Table 3 compares the dependability of the outcomes with those of Ishak *et al.* (2007) and Waini *et al.* (2020). The current findings align well with prior research. As a result, we are certain that the mathematical model that has been proposed is capable of accurately predicting the dynamic fluid flow behaviour for the purpose of this particular study.

Table 3: Results generation of $f''(0)$ with various S when $M = H = \vartheta = \phi_1 = \phi_2 = 0$

S	Current result	Waini *et al.* (2020)	Ishak *et al.* (2007)
0.00	1.232589	1.232588	1.2326
1.00	1.889313	1.889314	1.8893
−1.00	0.756577	0.756575	0.7566

Figure 2 depicts the effect of skin friction coefficient denoted by $f''(0)$ in relation to shrinking/stretching parameter λ as suction parameter, S $(S = 2.00, 2.10, 2.15)$ improves. The curves are solutions to boundary layer equations where the solid lines are referred to as "first solution" while the dashed lines are referred to as "second solution". This observation would indicate that the flow experiences a bifurcation region. Higher values of S correspond to stronger suction at the surface. From Figure 2, the graph trend of the skin friction coefficient $f''(0)$ is rised as S increases. It can be concluded that increasing the suction leads to an increase in the skin friction. Given boundary layer flow, as suction increases, the boundary layer thickness decreases. A decrease in boundary layer thickness reduces the capacity of fluid to transfer thereby exerting less shear stress at the surface which in turn leads to an increase in skin friction coefficient. The existence of multiple solutions perhaps implies the phenomenon of different boundary layer flow structures that can exist for the same set of conditions and could be associated with the transition of the flow between laminar and turbulent flow states or with other effects of stability. The dashed curves (second solution) may indicate of unstable flow regimes which are seldom found in practice.

Figure 3 shows the effect of suction on the heat transfer, described by $-\theta'(0)$ in a boundary layer flow. The graph depicts the relation between $-\theta'(0)$ and S. As presented in the graphs, it can be noted that with an increase in the value of S from 2.00, 2.10 to 2.15, there is a corresponding increase in the graph trend of $-\theta'(0)$. This implies that increased suction enhances heat transfer at the boundary layer of the shrinking wedge. The reason can be said to be due to the existence of thermal boundary layer. Suction not only enhances the thermal boundary layer but also transfers fluid from it, hence reducing its thickness. The heat flow is then enhanced as a greater amount of thermal energy is provided due to the increased difference in temperature between the cold and warm surfaces caused by the reduction in the thermal boundary layer thickness (high $-\theta'(0)$). In short, the addition of suction parameter enhances the effectiveness of the heat transfer from the surface.

At a constant value of $\lambda = -2.4$, different suction parameters S yield different velocity profiles $f'(\eta)$ as shown in Figure 4. The η axis, represents the dimensionless distance normal to the surface. An increase in the suction parameter S moves the velocity $f'(\eta)$

closer to the wall. In other words, the effect of S on the fluid is stronger, forcing the fluid at the surface to have a lower velocity. The fluid's momentum near the wall is reduced because of suction, which draws fluid away from the surface. This results in a thinner boundary layer and lower velocities closer to the surface. Moreover, the velocity profiles approach their asymptotic value progressively as the suction increases, and the thickness of the boundary layer is evidently reduced. Figure 5 demonstrates the temperature distributions $\theta(\eta)$ corresponding to different S when λ is kept constant at $\lambda = -2.4$. The behavior of the temperature profiles appears to be more intricate than the velocity profiles. The augmenting values of S resulting in lower temperature profile in the boundary layer flow, where the curves decline as S enhances. This is consistent with the previously stated phenomenon of thermal boundary layer thinning where it has been observed that a thinner thermal boundary layer increases the rate of heat transfer from the surface to the free stream and thus lowers the temperature next to the surface.

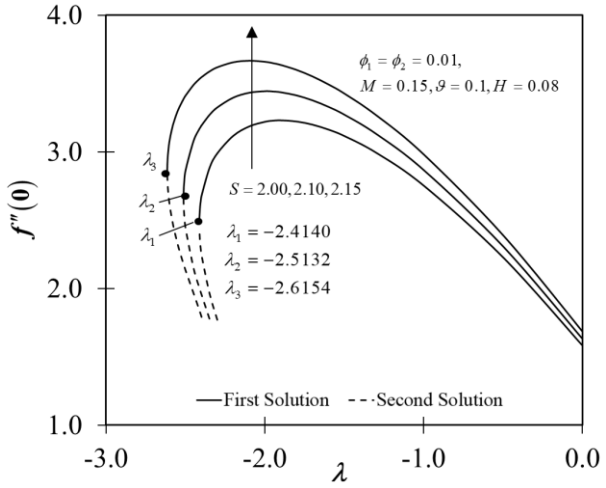

Figure 2: Variation of $f''(0)$ with several values of S

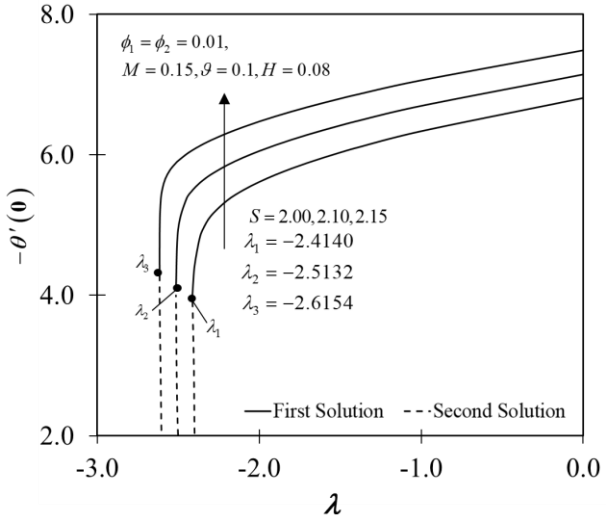

Figure 3: Variation of $-\theta'(0)$ with several values of S

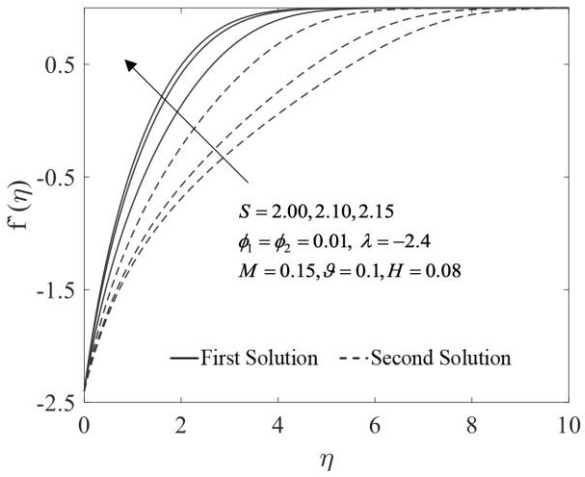

Figure 4: Variation of $f'(\eta)$ with several values of S

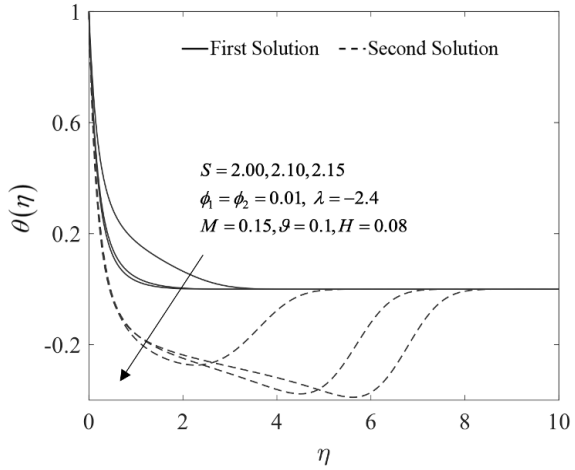

Figure 5: Variation of $\theta(\eta)$ with several values of S

Figure 6 shows how the wedge angle represented by parameter ϑ affects the skin friction coefficient, $f''(0)$. The parameter ϑ is directly proportional to β, where a higher value of ϑ corresponds to a larger wedge angle. As the wedge angle increases (indicated by increasing values of $\vartheta = 0.10, 0.15, 0.20$), the skin friction coefficient $f''(0)$ also increases with respect to λ. This means a larger wedge angle leads to a higher skin friction coefficient. The physical explanation lies in the boundary layer behavior. A larger wedge angle implies a more rapid increase in the external flow velocity along the wedge surface. This leads to a thicker boundary layer and a steeper velocity gradient near the surface. A steeper velocity gradient translates to a greater shear stress at the surface, which is directly proportional to the skin friction coefficient.

Figure 7 demonstrates the effect ϑ on the heat transfer rate, $-\theta'(0)$. As ϑ increases, $-\theta'(0)$ also increases towards λ. This means a larger wedge angle results in enhanced heat transfer at the surface. This behavior is related to the boundary layer thickness and the temperature gradient near the surface. A larger wedge angle leads to a higher external flow velocity and a thinner thermal boundary layer. A thinner thermal boundary layer means a

steeper temperature gradient at the surface, resulting in a higher heat transfer rate. This is similar to the impact of suction on heat transfer, except that the underlying mechanism is a change in external flow conditions caused by the wedge angle rather than surface mass transfer. The presence of both solution branches supports this characteristic, even if the second solution branch does not represent a physically feasible flow.

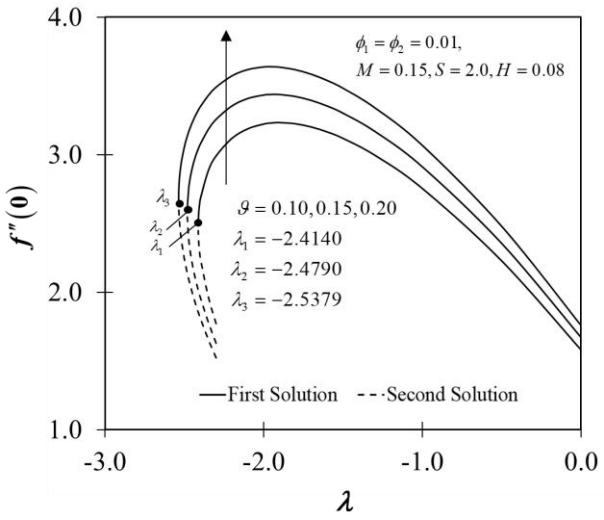

Figure 6: Variation of $f''(0)$ with several values of ϑ

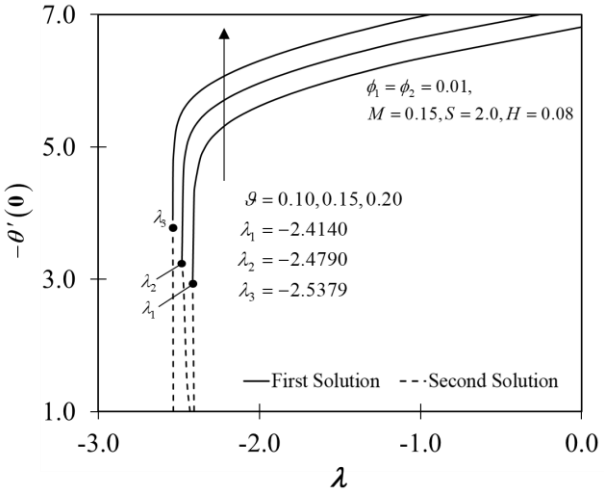

Figure 7: Variation of $-\theta'(0)$ with several values of ϑ

4. Conclusions

The findings reveal both suction and wedge angle significantly influence boundary layer flow characteristics. Increased suction reduces skin friction due to boundary layer thinning but enhances heat transfer based on a steeper temperature gradient. Concurrently, it decreases both velocity and temperature near the surface. Conversely, a larger wedge angle increases both skin friction and heat transfer. This is because the thermal boundary layer diminishes and the momentum boundary layer thickens, hence increasing shear stress as a result. The

persistent existence of multiple solutions over various parameters emphasises the flow's complexity and the possibility of flow instabilities, yet overall trends remain similar regardless of the solution branch.

Although this study provides valuable insights into the behavior of hybrid nanofluids, certain assumptions and limitations should be acknowledged. First, the hybrid nanofluid's thermophysical properties, such as nanoparticle size and thermal conductivity, are expected to be uniform, however aggregation and temperature dependency can change them. Second, while the numerical results have been confirmed against earlier studies, experimental validation is not included in this work to confirm the findings. In addition, this study focuses on steady-state conditions, neglecting transient effects that may arise in practical applications. to improve hybrid nanofluids' engineering and industrial applications, further studies should include experimental validation, analyse unsteady flow behaviours, and extend the model to more complex geometries.

Acknowledgements

The authors would like to express their appreciation to the Ministry of Higher Education (MoHE), Malaysia for the financial support (FRGS/1/2024/STG06/UTEM/03/1). Special thanks are also extended to Universiti Teknikal Malaysia Melaka (UTeM) for the continuous support and research facilities that made this work possible.

References

Abbasi A. & Farooq W. 2020. A numerical simulation for transport of hybrid nanofluid. *Arabian Journal for Science and Engineering* **45**(11): 9249-9265.

Atalık K & Sönmezler Ü. 2011. Heat transfer enhancement for boundary layer flow over a wedge by the use of electric fields. *Applied Mathematical Modelling* **35**(9): 4516-4525.

Awaludin I.S., Ishak A. & Pop I. 2018. On the stability of MHD boundary layer flow over a stretching/shrinking wedge. *Scientific Reports* **8**(1): 13622.

Crane L.J. 1970. Flow past a stretching plate. *Zeitschrift für angewandte Mathematik und Physik ZAMP* **21**: 645-647.

Ghosh S. & Mukhopadhyay S. 2022. Mixed convection flow of Cu-water nanofluid having differently shaped nanoparticles past a moving wedge. *Forces in Mechanics* **9**: 100149.

Guerrini L., Alvarez-Puebla R.A. & Pazos-Perez N. 2018. Surface modifications of nanoparticles for stability in biological fluids. *Materials* **11**(7): 1154.

Hartmann J. & Lazarus F. 1937. *Hg-dynamics*. Copenhagen: Levin & Munksgaard.

Heiser W.H. & Shercliff J.A. 1965. A simple demonstration of the Hartmann layer. *Journal of Fluid Mechanics* **22**(4): 701-707.

Ishak A., Nazar R. & Pop I. 2007. Falkner-Skan equation for flow past a moving wedge with suction or injection. *Journal of Applied Mathematics and Computing* **25**(1): 67-83.

Jin C., Wu Q., Yang G., Zhang H. & Zhong Y. 2021. Investigation on hybrid nanofluids based on carbon nanotubes filled with metal nanoparticles: Stability, thermal conductivity, and viscosity. *Powder Technology* **389**: 1-10.

Kakaç S. & Pramuanjaroenkij A. 2009. Review of convective heat transfer enhancement with nanofluids. *International Journal of Heat and Mass Transfer* **52**(13-14): 3187-3196.

Khan M.S., Mei S., Shabnam, Fernandez-Gamiz U., Noeiaghdam S., Shah S.A. & Khan A. 2022. Numerical analysis of unsteady hybrid nanofluid flow comprising CNTs-ferrousoxide/water with variable magnetic field. *Nanomaterials* **12**(2): 180.

Kolsi L., Adnan, Mir A., Muhammad T., Bilal M. & Ahmad Z. 2024. Numerical simulation of heat and mass transfer through hybrid nanofluid flow consists of polymer/CNT matrix nanocomposites across parallel sheets. *Alexandria Engineering Journal* **108**: 319-331.

Mahariq I., Khan D., Ghazwani H.A. & Shah M.A. 2024. Enhancing heat and mass transfer in MHD tetra hybrid nanofluid on solar collector plate through fractal operator analysis. *Results in Engineering* **24**: 103163.

Moreau R. 1990. The equations of magnetohydrodynamics. *Magnetohydrodynamics*: 1-31. Dordrecht: Kluwer Academic Publishers.

Nazari M.A., Ghasempour R., Ahmadi M.H., Heydarian G. & Shafii M.B. 2018. Experimental investigation of graphene oxide nanofluid on heat transfer enhancement of pulsating heat pipe. *International Communications in Heat and Mass Transfer* **91**: 90-94.

Oztop H.F. & Abu-Nada E. 2008. Numerical study of natural convection in partially heated rectangular enclosures filled with nanofluids. *International Journal of Heat and Fluid Flow* **29**(5): 1326-1336.

Pandey A.K. & Kumar M. 2016. Effect of viscous dissipation and suction/injection on MHD nanofluid flow over a wedge with porous medium and slip. *Alexandria Engineering Journal* **55**(4): 3115-3123.

Qureshi M.A., Hussain S. & Sadiq M.A. 2021. Numerical simulations of MHD mixed convection of hybrid nanofluid flow in a horizontal channel with cavity: Impact on heat transfer and hydrodynamic forces. *Case Studies in Thermal Engineering* **27**: 101321.

Raza J., Rohni A.M. & Omar Z. 2016. Numerical investigation of copper-water (Cu-water) nanofluid with different shapes of nanoparticles in a channel with stretching wall: Slip effects. *Mathematical and Computational Applications* **21**(4): 43.

Rohni A.M., Ahmad S. & Pop I. 2012. Flow and heat transfer over an unsteady shrinking sheet with suction in nanofluids. *International Journal of Heat and Mass Transfer* **55**(7-8): 1888-1895.

Sakiadis B.C. 1961. Boundary-layer behavior on continuous solid surfaces: II. The boundary layer on a continuous flat surface. *AiChE Journal* **7**(2): 221-225.

Sidik N.A.C., Jamil M.M., Japar W.M.A.A. & Adamu I.M. 2017. A review on preparation methods, stability and applications of hybrid nanofluids. *Renewable and Sustainable Energy Reviews* **80**: 1112-1122.

Sparrow E.M., Eckert E.R.G. & Minkowycz W.J. 1963. Transpiration cooling in a magneto-hydrodynamic stagnation-point flow. *Applied Scientific Research, Section A* **11**: 125-147.

Smrity A.M.A. & Yin P. 2024. Design and performance evaluation of pulsating heat pipe using metallic nanoparticles based hybrid nanofluids. *International Journal of Heat and Mass Transfer* **218**: 124773.

Tanveer A., Iram, Alqarni M.Z., Saleem S. & Al-Zubaidi A. 2025. Enhancement in heat generation through ternary hybrid nanofluid in a periodic channel. *Case Studies in Thermal Engineering* **69**: 106011.

Tiwari R.K. & Das M.K. 2007. Heat transfer augmentation in a two-sided lid-driven differentially heated square cavity utilizing nanofluids. *International Journal of Heat and Mass Transfer* **50**(9-10): 2002–2018.

Waini I., Ishak A. & Pop I. 2020. MHD flow and heat transfer of a hybrid nanofluid past a permeable stretching/shrinking wedge. *Applied Mathematics and Mechanics* **41**(3): 507-520.

Yu W., France D.M., Routbort J.L. & Choi S.U.S. 2008. Review and comparison of nanofluid thermal conductivity and heat transfer enhancements. *Heat Transfer Engineering* **29**(5): 432-460.

Zainal N.A., Waini I., Khashi'ie N.S., Nazar R. & Pop I. 2024. Thermal radiation effect on unsteady MHD rear stagnation point in Al_2O_3-Cu/H_2O hybrid nanofluids. *Journal of Quality Measurement and Analysis* **20**(1): 1–13.

Fakulti Teknologi dan Kejuruteraan Mekanikal
Universiti Teknikal Malaysia Melaka
Hang Tuah Jaya
Durian Tunggal 76100
Melaka, MALAYSIA
E-mail: nurulamira@utem.edu.my[*]

Department of Mathematical Sciences
Faculty of Science and Technology
Universiti Kebangsaan Malaysia
43600 UKM Bangi
Selangor, MALAYSIA
E-mail: rmn@ukm.edu.my

Department of Applied Mathematics
M. J. P. Rohilkhand University
Bareilly, 243006
Uttar Pradesh, INDIA
Email: haris.mjpru@gmail.com

Department of Mathematics
Babeş-Bolyai University
R-400084 Cluj-Napoca
ROMANIA
E-mail: popm.ioan@yahoo.co.uk

Received: 7 January 2025
Accepted: 19 March 2025

*Corresponding author